Kinetics and thermodynamics of T cell receptor–autoantigen interactions in murine experimental autoimmune encephalomyelitis

K. Christopher Garcia*†, Caius G. Radu†‡, Joseph Ho*, Raimund J. Ober§, and E. Sally Ward‡§¶

‡Center for Immunology and §Cancer Immunobiology Center, University of Texas Southwestern Medical Center, Dallas, TX 75390-8576; and *Departments of Microbiology and Immunology, and Structural Biology, Stanford University School of Medicine, Stanford, CA 94305-5124

Communicated by Hugh O. McDevitt, Stanford University School of Medicine, Stanford, CA, April 2, 2001 (received for review December 1, 2000)

In the current study, cellular and molecular approaches have been used to analyze the biophysical nature of T cell receptor (TCR)–peptide MHC (pMHC) interactions for two autoreactive TCRs. These two TCRs recognize the N-terminal epitope of myelin basic protein (MBP1–11) bound to the MHC class II protein, I-A^u, and are associated with murine experimental autoimmune encephalomyelitis. Mice transgenic for the TCRs have been generated and characterized in other laboratories. These analyses indicate that the mice either develop encephalomyelitis spontaneously (172.10 TCR) or only if immunized with autoantigen in adjuvant (1934.4 TCR). Here, we show that the 172.10 TCR binds MBP1–11:I-A^u with a 4–5-fold higher affinity than the 1934.4 TCR. Consistent with the higher affinity, 172.10 T hybridoma cells are significantly more responsive to autoantigen than 1934.4 cells. The interaction of the 172.10 TCR with cognate ligand is more entropically unfavorable than that of the 1934.4 TCR, indicating that the 172.10 TCR undergoes greater conformational rearrangements upon ligand binding. The studies therefore suggest a correlation between the strength and plasticity of a TCR–pMHC interaction and the frequency of spontaneous disease in the corresponding TCR transgenic mice. The comparative analysis of these two TCRs has implications for understanding autoreactive T cell recognition and activation.

Understanding the molecular basis of T cell recognition has been an area of intensive study, and during the last few years many of the details have emerged from structural and biochemical studies (1). However, there is a paucity of data describing the role of the biophysical details of the interactions of T cell receptors (TCRs) with peptide-MHC (pMHC) complexes in the pathogenesis of autoimmunity. In particular, the effect of variations in affinity and plasticity of autoreactive TCR–pMHC interactions on the onset and severity of disease is unknown. An additional unanswered question is whether the interaction of autoreactive TCRs with self-pMHC complexes resembles a TCR-foreign pMHC interaction with respect to the kinetics and thermodynamics of binding. Here, we investigate these issues by analysis of two autoreactive TCRs associated with the murine model of autoimmunity, experimental autoimmune encephalomyelitis (EAE) (2–4).

A distinguishing feature of the TCR interaction with pMHC, as compared with antibody–antigen interactions, is that TCRs bind their ligands with a relatively low affinity (5–7) and are more degenerate in their specificity (8–12). A deleterious practical manifestation of T cell crossreactivity is seen in autoimmune disorders such as multiple sclerosis, in which T cells mount an inflammatory immune response against neural self-antigens. In both multiple sclerosis and the animal model EAE, pathogenic T cells can be isolated with reactivity toward peptide fragments derived from myelin basic protein (MBP). The etiology of the autoreactive T cells remains controversial, but ''molecular mimicry'' of the self-pMHC by a structurally similar foreign pathogen has been proposed to account for the priming of the T cell (11, 13–16). Thus, degenerate recognition by autoreactive TCRs may play a role in the induction of autoimmunity.

Rather than being a simple on–off switch, TCR triggering involves a continuum of biochemical events that may frequently only result in partial T cell responses rather than full T cell activation (17, 18). Multiple studies with soluble recombinant molecules have indicated that the affinity, and particularly the off-rate, is a key determinant in the outcome of a TCR–pMHC interaction (7, 19–21). The characteristics of this tripartite interaction are that relative to the majority of other receptor–ligand interactions, it has a slow on-rate and a comparatively fast off-rate (1). The low on-rate suggests that some conformational rearrangement of TCR and/or pMHC is necessary for binding, consistent with studies demonstrating that the interaction is entropically unfavorable (22, 23). X-ray crystallographic analyses of tripartite TCR–pMHC interactions have shown poor shape complementarity and conformational changes by the TCR (24–29). This provides a mechanism of ''structural plasticity'' to widen the recognition repertoire of TCRs. Such plasticity or remodeling of the CDR loops of the TCR is consistent with crossreactivity, a known and apparently essential feature of T cell recognition (8–12).

In the current study, we have analyzed the interaction of two TCRs that are associated with murine EAE in H-2^u mice (3, 4) with their cognate ligand, MBP residues 1–11 (or core epitope, MBP1–9), bound to the MHC class II molecule, I-A^u. The TCRs (172.10 and 1934.4) are derived from encephalitogenic T cells isolated from MBP-immunized H-2^u mice (3, 4, 30). TCR transgenic (tg) mice have been generated for both TCRs and characterized in other laboratories (31–33). Interestingly, 172.10 tg mice succumb to spontaneous disease at a relatively high frequency (43%) (32, 34) when housed in nonspecific pathogen-free facilities. In contrast, unless immunized with MBP in adjuvant, 1934.4 tg mice are resistant to disease (31) even when backcrossed onto the same genetic background (B10.PL) as 172.10 tg mice (D. C Wraith and S.M. Anderton, personal communication). To better understand autoreactive T cell recognition in these tg models, we have carried out an analysis of the interaction of the 172.10 and 1934.4 TCRs with cognate ligand by using both soluble recombinant molecules and cell binding assays. The analyses suggest that the affinity and plasticity of a TCR–pMHC interaction may contribute to disease susceptibility in the tg mice, and these observations have implications for understanding how autoreactive T cells might be triggered to become pathogenic.

Abbreviations: EAE, experimental autoimmune encephalomyelitis; MBP, myelin basic protein; pMHC, peptide-MHC; SPR, surface plasmon resonance; TCR, T cell receptor; tg, transgenic; APC, antigen-presenting cell; PE, phycoerythrin.

†K.C.G. and C.G.R. contributed equally to this work.

¶To whom reprint requests should be addressed. E-mail: sally@skylab.swmed.edu.

The publication costs of this article were defrayed in part by page charge payment. This article must therefore be hereby marked "*advertisement*" in accordance with 18 U.S.C. §1734 solely to indicate this fact.

 www.pnas.org/cgi/doi/10.1073/pnas.111161198

Experimental Procedures

Cell Lines and Peptides. The 1934.4 and 172.10 hybridomas (4, 30) were generous gifts of Dr. David Wraith (1934.4), Dr. Vipin Kumar (172.10), and Dr. Joan Goverman (172.10). The I-A^u expressing cell lines, PL-8 (35) and Utm6.15 (36), were generously provided by Dr. David Wraith and Dr. Harden McConnell, respectively. The NH_2-terminal peptide MBP1–9 (acetylated at position 1) of mouse MBP and an analog in which lysine at position 4 is substituted by tyrosine were synthesized at the peptide synthesis unit of the Howard Hughes Medical Institute, UT Southwestern Medical Center.

Fluorescence-Activated Cell Sorting and Cloning of T Cell Hybridomas. TCR and CD4 expression levels on 1934.4 and 172.10 hybridoma cells were analyzed by using the following antibodies (all from PharMingen): H57–597 (anti-TCR, FITC labeled), F23.1 [anti-Vβ8, phycoerythrin (PE) labeled], and GK1.5 (anti-CD4, PE labeled). Fc Block (PharMingen) was used to block nonspecific binding. To isolate $TCR^{high}/CD4^{high}$ cells, 1934.4 and 172.10 hybridomas were labeled with H57–597 and GK1.5 antibodies and sorted twice by using a FACStar instrument (Immunocytometry Systems, San Jose, CA). Between the two rounds of sorting, cells were also subjected to magnetic cell separations by using anti-CD4 microbeads (Miltenyi Biotec, Auburn, CA). The purified $TCR^{high}/CD4^{high}$ populations were then cloned by limiting dilution.

T Cell Stimulation Assays. Triplicate cultures of T cell hybridomas (5×10^4 per well) were coincubated with the I-A^u expressing cells (5×10^4 per well), Utm6.15 (36), and different concentrations of MBP peptide. IL-2 levels were determined as described (37), by using recombinant murine IL-2 (PharMingen) to generate a standard curve.

Expression and Refolding of the TCRs. Single-chain VαVβ fragments (scTCRs), linked by $(Gly4Ser)_x$ linkers (12 residues for 172.10, 15 residues for 1934.4), were expressed in *Escherichia coli* in the pet28a vector (Novagen). Briefly, the 1934.4 (Vα4.2, Vβ8.2) or 172.10 (Vα2.3, Vβ8.2) scTCR gene was subcloned into the *Nde*I/*Eco*RI sites of pet28a, which placed the scTCRs in-frame with an N-terminal 6-His tag linked to the first residue of the scTCR through a thrombin-cleavable linker. Initially, genes encoding both wild-type and mutated scTCRs (residues Ile-75 and Leu-78 of the Vβ to Thr and Ser, respectively) were subcloned into the expression constructs. In earlier studies, these mutations were shown to improve the expression yield as soluble, secreted scTCRs from recombinant *E. coli* cells (E.S.W., unpublished results). The expression of the protein, by using *E. coli* BL21-plus (Stratagene) as host, was induced by addition of 1 mM isopropyl β-D-thiogalactoside. Inclusion bodies were purified by French press lysis and repeated washes with 1 M urea. In a typical refolding reaction, 100 mg of inclusion bodies of either scTCR were dissolved in 1 ml of 7 M GdHCl (1934.4) or 8 M urea (172.10) containing 10 mM DTT. This 1 ml was added to 200 ml of stirring 2 M GdHCl or 2 M urea containing 2 mM glutathione/0.2 mM glutathione disulfide at 4°C and stirred for 6 h. After 6 h, a dropwise addition of 50 mM Tris-HCl, pH 8.0, was initiated so that the refolding solution was diluted to 1.2 liters over 24 h and then allowed to stir for another 48 h. Recombinant scTCRs were purified by using Ni^{2+}-NTA-agarose (Qiagen, Chatsworth, CA) followed by gel filtration (Superdex 200, Amersham Pharmacia). For cleavage of the His-tag, the purified scTCR was passed through a thrombin column (bovine thrombin, Calbiochem) coupled to Affi-gel 15 (Bio-Rad) repeatedly until the N-terminal tag was completely removed. Peak scTCR fractions were pooled and concentrated to ≈10 mg/ml, sterile-filtered, and stored at 4°C. No evidence of aggregation was seen after storage for at least several months.

Expression of MBP1–11:I-A^u Complexes. Recombinant MBP1–11[4Y]:I-A^u complexes containing covalently tethered peptide were expressed in baculovirus-infected High Five cells (Invitrogen) as described (38). N-terminal acetylation of the MBP peptide can be replaced by an N-terminal glycine (as in the construct) without affecting T cell recognition (D. C. Wraith, personal communication). Position 4 substitution of the wild-type residue lysine by tyrosine increases the affinity of the peptide for I-A^u (36, 39, 40) but does not appear to affect the qualitative nature of T cell recognition (41, 42). A construct in which the codons encoding MBP1–11[4Y] were replaced by those encoding ovalbumin 323–339 was also generated. This peptide binds tightly to I-A^u (40). Purified proteins were biotinylated by using site-specific biotinylation with the enzyme BirA (Avidity, Denver, CO).

Analyses Using Surface Plasmon Resonance. All surface plasmon resonance (SPR) experiments were carried out on a BIAcore 2000. Flow cells on CM5 sensor chips were coupled with streptavidin by using amine-coupling chemistry to a density of ≈2,000 RU. Biotinylated MBP1–11[4Y]:I-A^u or Ova323–339:I-A^u complexes were loaded onto the streptavidin-coupled flow cells to varying densities. In some experiments, flow cells were treated with coupling buffer (10 mM sodium acetate, pH 4.8) only during the coupling cycle ("blank" flow cells). Data from blank flow cells or streptavidin-coupled flow cells were used as reference cells for subtraction of bulk shifts etc. Sensorgrams from these two types of reference cells essentially overlapped following zero adjustment. Flow rates of 10 μl/min (equilibrium binding experiments) and 20 μl/min (kinetic and temperature variation experiments) were used. The expression yield of the soluble pMHC complexes, together with the micromolar amounts needed, precluded SPR analyses by using these molecules as analyte. All experiments were carried out by using HBS buffer (BIAcore). Injections of analyte were carried out in duplicate by using the "kinject" command and programmed methods. Equilibrium binding experiments were performed at 25°C, and for the analysis of the effect of temperature, a range of temperatures from 10°C to 34°C (in 3°C increments) was used. Almost complete loss in binding activity of the 1934.4 scTCR occurred when the temperature was increased to 37°C, suggesting that this scTCR was unstable at this temperature. For this reason, data for this temperature were not used in the analyses. For equilibrium binding experiments, the concentrations of scTCRs ranged from ≈2–80 μM, and for analyses of the effect of temperature, a concentration of 8.5 or 10 μM (172.10 scTCR) or 38.4 μM (1934.4 scTCR) was used. The loss of activity of the MBP1–11[4Y]:I-A^u complexes on the flow cell during the course of the experiment was assessed by repeat injections of analyte at the end of the run of injections. For all data reported, loss in ligand activity was found to be negligible.

Data Processing. Data were zero adjusted, and reference cell data were subtracted before analysis. Equilibrium binding experiments were analyzed by using Scatchard plots. For kinetic analyses, data were fitted to a 1:1 interaction model (both BIAevaluation 2.2.4 and 3.0 software was used; on- and off-rates reported are determined by using BIAevaluation 2.2.4 software). The accuracy of off-rate determinations was limited by the fast dissociation of the TCRs from immobilized ligand, particularly when the temperature of the interaction was 25°C or higher. Two approaches were taken in an attempt to derive kinetic constants as close to the "true" values as possible. First, data obtained from sensor flow cells coupled with low density of ligand (711 RU) were used to minimize effects due to mass transport and

rebinding (43). Second, artifacts in kinetic constants introduced by reference cell subtraction were reduced by using the same reference cell on the sensor chip during data analyses (44).

For analysis of the effects of temperature on the affinity of the TCR–pMHC interactions, the dissociation constant (K_D) at each temperature was calculated by analyzing the amount bound at equilibrium by using the equation: $R_{eq} = R_{max} \times [TCR]/(K_D + [TCR])$, where R_{eq} = amount bound (expressed in RU) at equilibrium, R_{max} = maximum binding capacity of chip, [TCR] = concentration of TCR, and K_D = dissociation constant. Equilibrium experiments were used in preference to kinetic experiments to determine K_D values, as equilibrium values are less susceptible to mass transport and rebinding effects (43). It was possible to derive K_D values from Req values for different interaction temperatures as although the effect of temperature on absolute RU value in SPR experiments is dramatic, analysis of the bulk shifts in control flow cells following zero adjustment of the sensorgrams indicated that they did not differ significantly (data not shown). The zero-adjusted and reference cell-subtracted R_{eq} values from the analyses at different temperatures can therefore reliably be used to determine equilibrium binding affinities. K_D values were then used to calculate the free energy change, ΔG^o. ΔG^o vs. temperature plots were fitted by using linear regression as described (23).

Binding of MBP1–11:I-A^u Tetramers to 172.10 and 1934.4 Hybridomas. Tetramer staining was carried out for 30 min at 12°C and 37°C by using previously described methods (38) with the following modifications: sodium azide (0.01%) was added to the staining buffer, and the anti-CD3ε antibody, 145–2C11, was omitted.

Results

Antigen Responsiveness of the 172.10 and 1934.4 Hybridoma Cells. Initially, a direct comparison of IL-2 secretion levels by T hybridoma cells bearing the 172.10 and 1934.4 TCRs was made by using peptide-pulsed antigen-presenting cells (APC) as the stimulant. However, the instability of both TCR and CD4 expression levels by the 172.10 hybridoma cells (J. Goverman, personal communication, and our observations) necessitated the sorting of these cells into TCR^{high}CD4^{high} populations before analysis. Although the TCR and CD4 expression levels on the 1934.4 hybridoma cells are more stable, for comparative purposes these were also sorted and cloned. TCR/CD4 expression levels for representative clones are shown in Fig. 1*A*. The CD4 expression levels are similar, but the 1934.4 cells express significantly higher levels of TCR than 172.10 cells. Both the wild-type peptide, MBP1–9, and a position 4 analog (lysine substituted by tyrosine, 4Y), which binds to I-A^u with higher affinity (36, 39, 40), were used in the stimulation assays. 172.10 cells are significantly more responsive than 1934.4 cells to both antigens despite the lower levels of TCR expression levels (Fig. 1*B*). These differences were seen for both the sorted populations and cloned cells (Fig. 1*B* and data not shown) and were particularly marked for the wild-type peptide, MBP1–9, which, because of its lower affinity for I-A^u relative to the position 4 analog 4Y, results in a lower antigen density on the surface of pulsed APCs. The patterns of antigen responsiveness, together with the differences in disease susceptibility of 172.10 and 1934.4 tg mice (31, 32), prompted us to carry out biophysical analyses of the corresponding TCR–pMHC interactions.

Determination of the Affinity and Kinetics of the TCR–pMHC Interactions. To investigate the TCR–pMHC interactions of the 172.10 and 1934.4 T cells in molecular detail, scTCRs were produced in *E. coli* as soluble, refolded VαVβ heterodimers. Earlier studies with soluble, secreted scTCRs had shown that mutation of two surface-exposed, hydrophobic residues (Ile-75, Leu-78) on the Vβ8.2 domain (45, 46) to hydrophilic residues (Thr-75, Ser-78)

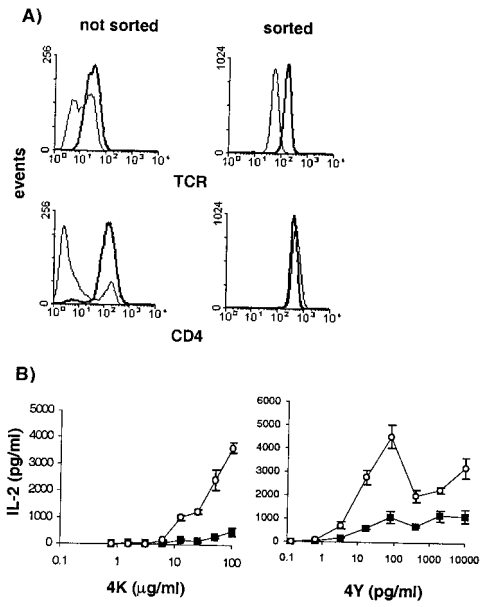

Fig. 1. (*A*) The TCR and CD4 levels on the 1934.4 (thick lines) and 172.10 (thin lines) T cell hybridomas before and after sorting followed by cloning. Cells were stained with H57–597 (FITC-labeled) and GK1.5 (PE-labeled) and analyzed by flow cytometry. Data for one representative clone are shown. (*B*) IL-2 secretion by the 1934.4 (■) and 172.10 (○) hybridoma cells in response to Utm6.15 cells pulsed with antigenic peptides (4K, wild-type MBP1–9 peptide; 4Y, MBP analog with position 4 lysine substituted by Tyr). Data for one representative clone are shown, and similar results were obtained for sorted, uncloned cells and PL-8 cells (35) as APCs (not shown). Results are representative of three independent experiments.

resulted in improved expression yields (E.S.W., unpublished results). Refolding followed by gel filtration of scTCRs harboring these two mutations resulted in protein of the correct size that was soluble at >15 mg/ml (Fig. 2). In contrast, the wild-type scTCRs tended to aggregate at concentrations >1 mg/ml. Thus, the mutated scTCRs were used in binding studies. Importantly, the mutations are located distal to the putative antigen binding site and are not expected to affect the binding of the scTCRs to ligand (Fig. 2).

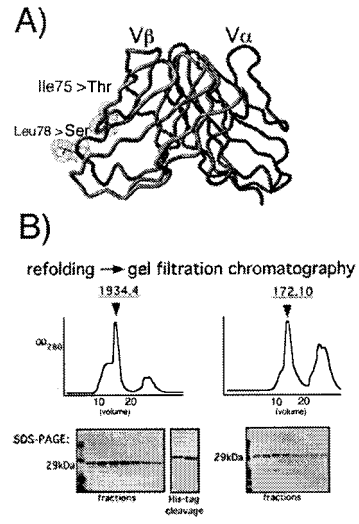

Fig. 2. (*A*) The location of solubility-enhancing mutations indicated on the crystal structure of the 2C TCR (Vβ8.2) (46). (*B*) Purification of the refolded scTCRs.

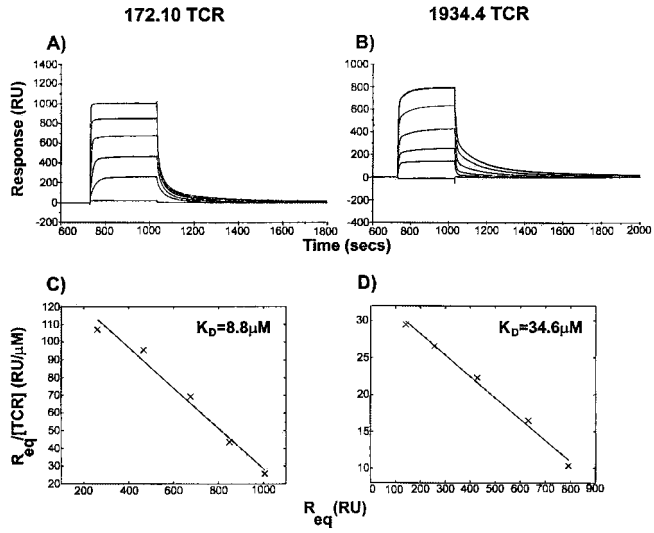

Fig. 3. Equilibrium binding analyses of 172.10 (*A*) and 1934.4 (*B*) scTCRs. Flow cells of a CM5 sensor chip were coupled to a density of 3,076 RU (MBP1–11[4Y]:I-A^u, 1975 RU (Ova323–339:I-A^u) or treated with buffer only during the coupling cycle. Overlays of duplicate injections of scTCRs at 10 μl/min following zero adjustment and reference cell data subtraction are shown. The lowest level trace represents the binding of 172.10 scTCR (39 μM) or 1934.4 scTCR (76.8 μM) to Ova323–339:I-A^u. scTCR concentrations for sensorgrams showing binding to MBP1–11[4Y]:I-A^u (R_{eq} values in parentheses) were as follows: (*A*) 39 μM (1005.2), 19.5 μM (848.9), 9.76 μM (676.3), 4.88 μM (466.1), and 2.44 μM (261.0); (*B*) 76.8 μM (791.9), 38.4 μM (632.5), 19.2 μM (428.5), 9.6 μM (255.0), and 4.8 μM (141.6). *C* and *D* show the Scatchard analyses corresponding to *A* and *B*, respectively.

The binding of the 1934.4 and 172.10 scTCRs to immobilized MBP1–11[4Y]:I-A^u was analyzed at 25°C by using SPR. MBP1–11[4Y]:I-A^u complexes were site-specifically biotinylated (38) and coupled to streptavidin sensor chips. Equilibrium binding analyses demonstrated that the dissociation constants (K_D) of these TCRs are 34.6 μM (1934.4) and 8.8 μM (172.10) (Fig. 3). Binding to immobilized Ova323–339:I-A^u was at almost background levels for the highest concentrations of scTCR used, demonstrating that the scTCRs are highly specific for cognate ligand (Fig. 3).

The kinetics of the interactions at 25°C were also investigated (Table 1). In these SPR experiments, relatively low coupling densities of immobilized ligand (711 RU MBP1–11[4Y]:I-A^u) were used to minimize mass transport and rebinding effects (43). Indeed, the use of high coupling densities (about 3,000 RU of MBP1–11[4Y]:I-A^u) resulted in significant slowing of the apparent on- and off-rates (Fig. 3, not shown). Despite the higher equilibrium binding affinity of the 172.10 scTCR compared with that of the 1934.4 scTCR, the off-rate is slightly faster for the 172.10 scTCR (Table 1). The high on-rate of this scTCR, which is about 7-fold faster than that of the 1934.4 scTCR, therefore compensates for its faster off-rate, which in turn results in a higher affinity.

Table 1. Kinetic constants of the TCR–pMHC interactions

TCR	k_{on} (mol^{-1} s^{-1})*	k_{off} (s^{-1})*	K_D (μM)
172.10	3.72×10^4	0.219	5.9
1934.4	5.13×10^3	0.160	31

Kinetic constants were determined by using 10 μM 172.10 TCR or 38.4 μM 1934.4 TCR and a coupling density of 711 RU MBP1-11[4Y]:I-A^u.

*Values are averages from two analyte (TCR) injections; standard errors were less than 7.2% for individual estimates.

The Thermodynamics of the TCR–pMHC Interactions. Analyses of the temperature dependence of the affinity and kinetics of protein–protein complexation can yield information concerning the thermodynamics of the interaction (22, 23). To investigate the effect of temperature on 1934.4 and 172.10 scTCR binding to cognate ligand, the interactions were therefore analyzed as the temperature was raised from 10° to 34°C in 3°C increments.

The sensorgrams in Fig. 4 show an increase in the on- and off-rates of the interactions for both scTCRs as the temperature is increased. In addition, the low ligand-coupling densities used in these experiments resulted in faster kinetics than those seen in the equilibrium binding analyses in Fig. 3. At temperatures above 25°C and by using these low-coupling densities, the off-rates are too fast to accurately estimate (44). For this reason, "equilibrium" rather than "kinetic" binding affinities for each temperature were derived from the sensorgrams. The dissociation constants were used to calculate the free energy change, ΔG^o, for each temperature, and ΔG^o vs. temperature plots are shown in Fig. 4 *C* and *D*. A difference in behavior of the two scTCRs at temperatures below 22°C (295K) is apparent. The differences in curvature and slope result in different estimates for the standard enthalpies, heat capacities, and entropies of the scTCR–pMHC interactions (Table 2).

Binding of MBP1–11:I-A^u Tetramers to the 1934.4 and 172.10 T Cell Hybridomas. Recombinant MBP1–11:I-A^u tetramers (38) were used to correlate the *in vitro* binding data obtained by using SPR with the interaction of native, cell surface-bound TCR with cognate ligand. In several studies, the level of tetramer staining has been shown to correlate with the affinity of the TCR for ligand (47, 48). Tetramer staining was carried out with sorted, cloned 1934.4 and 172.10 T hybridoma cells at 12°C and 37°C (Fig. 5). To allow a comparison of tetramer binding to be made,

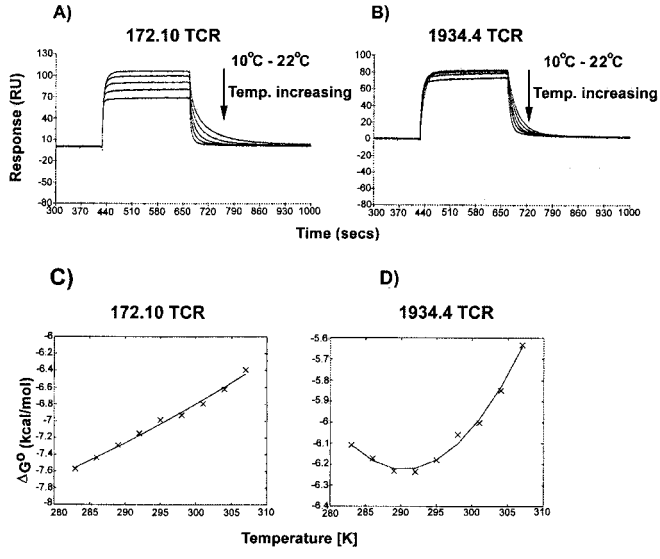

Fig. 4. Effect of temperature on the scTCR–pMHC ligand interactions. 172.10 scTCR (*A*) or 1934.4 scTCR (*B*) were injected at 20 μl/min at concentrations of 8.5 μM (*A*) or 38.4 μM (*B*). Temperatures of 10, 13, 16, 19, and 22°C (*A* and *B*) or 25, 28, 31, and 34°C (not shown) were used. Flow cells of CM5 chips were coupled with biotinylated MBP1–11[4Y]:I-A^u to a density of 435 RU. The arrow indicates the decrease in R_{eq} values as the temperature was increased. For the 1934.4 scTCR, effects on R_{eq} were negligible for a temperature increase from 10°C to 16°C (*B*), although effects on the kinetics could be seen. Overlays of duplicate injections following zero adjustment and reference cell data subtraction are shown. (*C* and *D*) Plots of ΔG^o vs. temperature (in Kelvin). These curves were fitted as described (23) to derive the thermodynamic parameters shown in Table 2.

Table 2. Thermodynamic parameters for the TCR–pMHC interactions

TCR	ΔG° (kcal/mol)	ΔH° (kcal/mol)	TΔS° (kcal/mol)	ΔCp° (cal/mol/deg)
172.10	−6.9	−21.2	−14.3	−159
1934.4	−6.0	−15.7	−9.6	−1248

staining levels by the anti-Vβ8.2 antibody F23.1 were also determined at these temperatures, as the two T cell hybridomas express different levels of TCR (Fig. 1). These data are therefore represented as the ratio of tetramer staining to F23.1 staining at each temperature (Fig. 5*B*), which effectively normalizes the tetramer binding for TCR levels (47). Significantly, 172.10 T cells stain to higher levels with the tetramer than 1934.4 T cells (Fig. 5*B*). In addition, the normalized tetramer staining increases as the temperature is decreased, concordant with the increase in affinity of the TCR–pMHC interactions with decreasing temperature in the SPR experiments (Fig. 4).

Discussion

In the current study, we have analyzed the interaction of two recombinant scTCRs with the N-terminal epitope of MBP associated with I-A^u. These TCRs are derived from autoreactive T cells associated with the murine disease model, EAE. At physiological temperatures, the 172.10 TCR has an approximately 4-fold higher affinity than the 1934.4 TCR. This higher affinity is due to a 7-fold higher on-rate, which is counteracted by a slightly faster off-rate. The association rate of the 172.10 TCR falls at the high end of the range reported for TCRs (5, 7, 19–22). Taken together with the observation that 1934.4 hybridoma cells are significantly less responsive to antigen than 172.10 cells, this suggests that the high on-rate of the 172.10 TCR may compensate for the faster off-rate by enhancing rebinding at the T cell–APC interface. Hence, we observe an alternative mechanism of enhancing T cell responsiveness: through an increase in on-rate, as opposed to the decrease in off-rate reported in other systems (7, 19–21). The correlation between off-rate and responsiveness may therefore break down if the TCR–pMHC interaction under consideration has a relatively fast association rate.

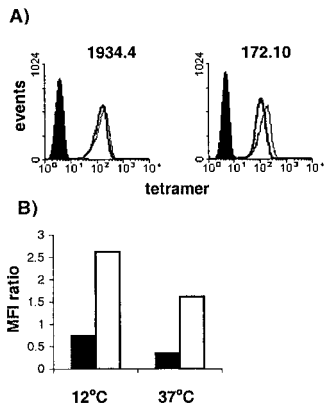

Fig. 5. (*A*) Binding of MBP1–11[4Y]:I-A^u tetramers to 1934.4 and 172.10 T cell hybridomas. Cells were incubated with PE-labeled tetramers for 30 min at 12°C (thick lines) and 37°C (thin lines), washed, and analyzed by flow cytometry. (*B*) Mean fluorescence intensity (MFI) ratio of PE-labeled tetramer to PE-labeled F23.1 binding to 1934.4 (filled bars) and 172.10 (open bars). Cells (20,000 events) were analyzed as in *A*, and MFI was determined by using the software WinMDI 2.8 (J. Trotter, Scripps Research Institute, La Jolla, CA). Results are representative of three independent experiments.

Interestingly, mice transgenic for the 172.10 TCR succumb to spontaneous EAE (32), whereas this is not observed for 1934.4 TCR tg mice (31) even when the tg mice are backcrossed onto the same (B10.PL) background (D. C. Wraith and S. M. Anderton, personal communication). Although we have analyzed only two TCRs, this suggests that spontaneous disease may be more common in tg models of autoimmunity where the TCR is of high affinity. This is consistent with the observations of others for EAE development in TCR tg SJL mice (49) and for autoreactive CD8+ T cells associated with the progression to overt diabetes in (nontransgenic) NOD mice (50). However, in these studies (49, 50), the thermodynamics and kinetics of the corresponding TCR–pMHC interactions were not analyzed. Thus, our study provides detailed molecular insight into the characteristics of an autoreactive TCR–pMHC interaction that may predispose toward pathogenesis when the TCR is expressed as a transgene. Because of the limited number of TCRs that we have analyzed, we cannot extrapolate our findings with certainty to other autoimmune systems. Murine EAE is one of the few autoimmune models currently available possessing transgenics with different disease susceptibilities that can subsequently be correlated with cellular and biochemical measurements.

In addition to the higher affinity and plasticity of the 172.10 TCR, the differences in disease susceptibility between the 172.10 and 1934.4 tg mice may be due to other, not mutually exclusive, factors. These include variations in the number of regulatory T cells, TCR expression levels, or numbers of backcrosses onto the B10.PL background. In this context, regulatory T cells have recently been shown to be essential in the prevention of a high incidence of spontaneous disease in tg models of EAE (51, 52). Significantly, spontaneous disease occurs with higher incidence in 172.10 tg mice housed in nonspecific pathogen-free facilities relative to specific pathogen-free facilities (32, 34) and has been shown to occur after infection with several different pathogens (34). Although this is suggestive of a mechanism involving molecular mimicry (11, 13, 14), this is made improbable by the observation that infection of 172.10 tg mice with different bacteria induces disease, but the responding autoreactive T cells are not stimulated by the pathogen (34). Taken together, the data suggest that infection may alter the cytokine or chemokine balance in the tg mice, which in turn results in triggering, possibly by crossreactive recognition, of the 172.10 tg T cells and/or their trafficking into the CNS. In contrast, by virtue of the lower affinity and plasticity of their TCR for cognate ligand, the 1934.4 tg cells may have a higher activation threshold and be less susceptible to crossreactive stimulation.

The differences in thermodynamic properties of the interactions of the 1934.4 and 172.10 TCRs with MBP1–11:I-A^u are of interest, particularly as the recognition specificity of these TCRs has been analyzed in detail (53). The T cell contacts for this MBP epitope are glutamine at position 3 and proline at position 6 (30, 54). Substitution of these positions with other amino acids has differential effects on recognition by short-term T cell lines derived from the 1934.4 and 172.10 tg mice (53). The two TCRs have different primary and secondary contacts, and the 172.10 TCR is more crossreactive. Relative to 1934.4 TCR–pMHC complexation, the 172.10 TCR–pMHC interaction is significantly less favorable in entropic terms. Taken together with the higher crossreactivity of this TCR, this indicates that the 172.10 binding surface is more plastic. Indeed, the presence of multiple glycines in the 172.10 CDR3β (4) could result in high flexibility in this region of the TCR. The effects of temperature on the TCR–pMHC interactions in the current study are reminiscent of those observed in analyses in which the binding of TCRs to foreign antigens was analyzed (22, 23). Thus, there are no fundamental differences at the molecular level between self and non-self recognition by T cells, and unfavorable entropic terms may be a general phenomenon for TCR–pMHC interactions.

The current study describes the characteristics, in molecular terms, of two TCR–autoantigen interactions. Unexpectedly, despite the significantly higher affinity of the 172.10 TCR relative to the 1934.4 TCR, it shows greater plasticity and crossreactivity. The plasticity of this TCR correlates with the highly unfavorable entropy of the TCR–ligand interaction and is concordant with a high degree of variation of affinity with temperature. The high adaptability, together with relatively high affinity, would seem to be in opposition to each other. T cells bearing TCRs with these properties may be unusually sensitive to priming by self-antigens, and as a consequence these recognition properties may be overrepresented in autoreactive, pathogenic T cells.

We are indebted to Darla Eaken for maintenance of the BIAcore 2000 instrument used in these studies and to Dr. Bertram Ober for optimization of the GlySer linker length for expression of the 1934.4 scTCR. We are grateful to Angie Mobley and Jik Ungchusri (Dallas Cell Analysis Facility) for expert assistance with the FACS. K.C.G. is grateful to Drs. Hugh McDevitt and Larry Steinman for helpful discussions. This work was supported by National Institutes of Health Grants R01 AI/NS42949 and R01 GM58538 (to E.S.W.) and RO1 AI54840 (to K.C.G.), National Multiple Sclerosis Society Grants RG-2411 (to E.S.W.) and RG-3148-A-1 (to K.C.G.), a grant from the Yellow Rose Foundation (to E.S.W), March of Dimes Grant 5-FY99-759 (to K.C.W.), and a grant from the Rita Allen Foundation (to K.C.G). The BIAcore 2000 was purchased through a shared National Institutes of Health equipment grant (to E.S.W.).

1. Davis, M. M., Boniface, J. J., Reich, Z., Lyons, D., Hampl, J., Arden, B. & Chien, Y. (1998) *Annu. Rev. Immunol.* **16,** 523–544.
2. Zamvil, S. S., Mitchell, D. J., Moore, A. C., Kitamura, K., Steinman, L. & Rothbard, J. B. (1986) *Nature (London)* **324,** 258–260.
3. Acha-Orbea, H., Mitchell, D. J., Timmermann, L., Wraith, D. C., Tausch, G. S., Waldor, M. K., Zamvil, S. S., McDevitt, H. O. & Steinman, L. (1988) *Cell* **54,** 263–273.
4. Urban, J. L., Kumar, V., Kono, D. H., Gomez, C., Horvath, S. J., Clayton, J., Ando, D. G., Sercarz, E. E. & Hood, L. (1988) *Cell* **54,** 577–592.
5. Corr, M., Slanetz, A. E., Boyd, L. F., Jelonek, M. T., Khilko, S., al-Ramadi, B. K., Kim, Y. S., Maher, S. E., Bothwell, A. L. & Margulies, D. H. (1994) *Science* **265,** 946–949.
6. Matsui, K., Boniface, J. J., Reay, P. A., Schild, H., Fazekas de St. Groth, B. & Davis, M. M. (1991) *Science* **254,** 1788–1791.
7. Matsui, K., Boniface, J. J., Steffner, P., Reay, P. A. & Davis, M. M. (1994) *Proc. Natl. Acad. Sci. USA* **91,** 12862–12866.
8. Bhardwaj, V., Kumar, V., Geysen, H. M. & Sercarz, E. E. (1993) *J. Immunol.* **151,** 5000–5010.
9. Reay, P. A., Kantor, R. M. & Davis, M. M. (1994) *J. Immunol.* **152,** 3946–3957.
10. Kersh, G. J. & Allen, P. M. (1996) *J. Exp. Med.* **184,** 1259–1268.
11. Wucherpfennig, K. W. & Strominger, J. L. (1995) *Cell* **80,** 695–705.
12. Mason, D. (1998) *Immunol. Today* **19,** 395–404.
13. Oldstone, M. B. (1987) *Cell* **50,** 819–820.
14. Hemmer, B., Fleckenstein, B. T., Vergelli, M., Jung, G., McFarland, H., Martin, R. & Wiesmuller, K. H. (1997) *J. Exp. Med.* **185,** 1651–1659.
15. Ufret-Vincenty, R. L., Quigley, L., Tresser, N., Pak, S. H., Gado, A., Hausmann, S., Wucherpfennig, K. W. & Brocke, S. (1998) *J. Exp. Med.* **188,** 1725–1738.
16. Gautam, A. M., Liblau, R., Chelvanayagam, G., Steinman, L. & Boston, T. (1998) *J. Immunol.* **161,** 60–64.
17. Sloan-Lancaster, J. & Allen, P. M. (1996) *Annu. Rev. Immunol.* **14,** 1–27.
18. Germain, R. N. & Stefanova, I. (1999) *Annu. Rev. Immunol.* **17,** 467–522.
19. Alam, S. M., Travers, P. J., Wung, J. L., Nasholds, W., Redpath, S., Jameson, S. C. & Gascoigne, N. R. (1996) *Nature (London)* **381,** 616–620.
20. Lyons, D. S., Lieberman, S. A., Hampl, J., Boniface, J. J., Chien, Y., Berg, L. J. & Davis, M. M. (1996) *Immunity* **5,** 53–61.
21. Kersh, G. J., Kersh, E. N., Fremont, D. H. & Allen, P. M. (1998) *Immunity* **9,** 817–826.
22. Willcox, B. E., Gao, G. F., Wyer, J. R., Ladbury, J. E., Bell, J. I., Jakobsen, B. K. & van der Merwe, P. A. (1999) *Immunity* **10,** 357–365.
23. Boniface, J. J., Reich, Z., Lyons, D. S. & Davis, M. M. (1999) *Proc. Natl. Acad. Sci. USA* **96,** 11446–11451.
24. Garboczi, D. N., Ghosh, P., Utz, U., Fan, Q. R., Biddison, W. E. & Wiley, D. C. (1996) *Nature (London)* **384,** 134–141.
25. Garcia, K. C., Degano, M., Pease, L. R., Huang, M., Peterson, P. A., Teyton, L. & Wilson, I. A. (1998) *Science* **279,** 1166–1172.
26. Ding, Y. H., Baker, B. M., Garboczi, D. N., Biddison, W. E. & Wiley, D. C. (1999) *Immunity* **11,** 45–56.
27. Degano, M., Garcia, K. C., Apostolopoulos, V., Rudolph, M. G., Teyton, L. & Wilson, I. A. (2000) *Immunity* **12,** 251–261.
28. Reinherz, E. L., Tan, K., Tang, L., Kern, P., Liu, J., Xiong, Y., Hussey, R. E., Smolyar, A., Hare, B., Zhang, R., *et al.* (1999) *Science* **286,** 1913–1921.
29. Garcia, K. C. (1999) *Immunol. Rev.* **172,** 73–85.
30. Wraith, D. C., Smilek, D. E., Mitchell, D. J., Steinman, L. & McDevitt, H. O. (1989) *Cell* **59,** 247–255.
31. Liu, G. Y., Fairchild, P. J., Smith, R. M., Prowle, J. R., Kioussis, D. & Wraith, D. C. (1995) *Immunity* **3,** 407–415.
32. Goverman, J., Woods, A., Larson, L., Weiner, L. P., Hood, L. & Zaller, D. M. (1993) *Cell* **72,** 551–560.
33. Pearson, C. I., van Ewijk, W. & McDevitt, H. O. (1997) *J. Exp. Med.* **185,** 583–599.
34. Goverman, J. (1999) *Immunol. Rev.* **169,** 147–159.
35. Wraith, D. C., Smilek, D. E. & Webb, S. (1992) *J. Autoimmun.* **5,** 103–113.
36. Mason, K., Denney, D. W. J. & McConnell, H. M. (1995) *J. Immunol.* **154,** 5216–5227.
37. Qadri, A., Radu, C. G., Thatte, J., Cianga, P., Ober, B. T., Ober, R. J. & Ward, E. S. (2000) *J. Immunol.* **165,** 820–829.
38. Radu, C., Anderton, S. M., Firan, M., Wraith, D. C. & Ward, E. S. (2000) *Int. Immunol.* **12,** 1553–1560.
39. Fairchild, P. J., Wildgoose, R., Atherton, E., Webb, S. & Wraith, D. C. (1993) *Int. Immunol.* **5,** 1151–1158.
40. Fugger, L., Liang, J., Gautam, A., Rothbard, J. B. & McDevitt, H. O. (1996) *Mol. Med.* **2,** 181–188.
41. Wraith, D. C., Bruun, B. & Fairchild, P. J. (1992) *J. Immunol.* **149,** 3765–3770.
42. Lee, C., Liang, M. N., Tate, K. M., Rabinowitz, J. D., Beeson, C., Jones, P. P. & McConnell, H. M. (1998) *J. Exp. Med.* **187,** 1505–1516.
43. Schuck, P. (1997) *Curr. Opin. Biotechnol.* **8,** 498–502.
44. Ober, R. J. & Ward, E. S. (1999) *Anal. Biochem.* **271,** 70–80.
45. Bentley, G. A., Boulot, G., Karjalainen, K. & Mariuzza, R. A. (1995) *Science* **267,** 1984–1987.
46. Garcia, K. C., Degano, M., Stanfield, R. L., Brunmark, A., Jackson, M. R., Peterson, P. A., Teyton, L. & Wilson, I. A. (1996) *Science* **274,** 209–219.
47. Crawford, F., Kozono, H., White, J., Marrack, P. & Kappler, J. (1998) *Immunity* **8,** 675–682.
48. Savage, P. A., Boniface, J. J. & Davis, M. M. (1999) *Immunity* **10,** 485–492.
49. Waldner, H., Whitters, M. J., Sobel, R. A., Collins, M. & Kuchroo, V. K. (2000) *Proc. Natl. Acad. Sci. USA* **97,** 3412–3417.
50. Amrani, A., Verdaguer, J., Serra, P., Tafuro, S., Tan, R. & Santamaria, P. (2000) *Nature (London)* **406,** 739–742.
51. Olivares-Villagomez, D., Wang, Y. & Lafaille, J. J. (1998) *J. Exp. Med.* **188,** 1883–1894.
52. Van de Keere, F. & Tonegawa, S. (1998) *J. Exp. Med.* **188,** 1875–1882.
53. Anderton, S. M., Manickasingham, S. P., Burkhart, C., Luckcuck, T. A., Holland, S. J., Lamont, A. G. & Wraith, D. C. (1998) *J. Immunol.* **161,** 3357–3364.
54. Gautam, A. M., Lock, C. B., Smilek, D. E., Pearson, C. I., Steinman, L. & McDevitt, H. O. (1994) *Proc. Natl. Acad. Sci. USA* **91,** 767–771.